Science of the Total Environment 720 (2020) 137539

Contents lists available at ScienceDirect

Science of the Total Environment

journal homepage: www.elsevier.com/locate/scitotenv

The sensitivity of the carbon sink by coupled carbonate weathering to climate and land-use changes: Sediment records of the biological carbon pump effect in Fuxian Lake, Yunnan, China, during the past century

Haibo He [a,b], Zaihua Liu [a,c,*], Chongying Chen [a], Yu Wei [a,b], Qian Bao [a,b], Hailong Sun [a], Hao Yan [a]

[a] State Key Laboratory of Environmental Geochemistry, Institute of Geochemistry, CAS, Guiyang 550081, Guizhou, China
[b] University of Chinese Academy of Sciences, Beijing 100049, China
[c] CAS Center for Excellence in Quaternary Science and Global Change, 710061 Xi'an, China

HIGHLIGHTS

- The ratios of AOC were determined by n-alkanes compound calculation.
- They ranged from 47 to 84%, with an average of 63%.
- The post-1950 AOC burial rate was about 7 times that for the period before.
- The sharp increase in the burial rate was chiefly related to land-use changes.
- It may contribute significantly to the missing sink in the global carbon cycle.

GRAPHICAL ABSTRACT

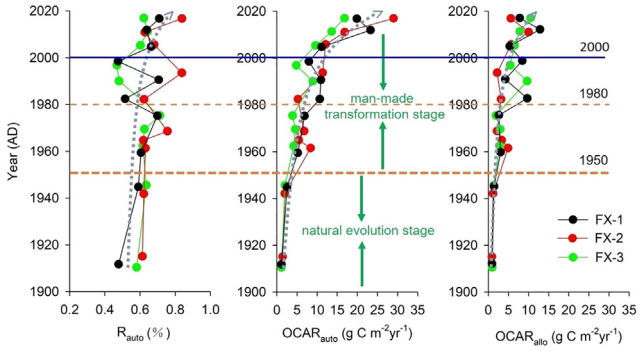

ARTICLE INFO

Article history:
Received 18 July 2019
Received in revised form 27 January 2020
Accepted 23 February 2020
Available online 26 February 2020

Editor: G. Darrel Jenerette

Keywords:
Coupled carbonate weathering
Biological carbon pump effect
Autochthonous organic carbon
Carbon sink
Climate change
Land-use change
Lake sedimentation

ABSTRACT

Recent studies show that the carbon sink attributable to the weathering of carbonate rocks may have been greatly underestimated if the biological carbon pump (BCP) effect in transferring dissolved inorganic carbon (DIC) to organic carbon (autochthonous OC) by aquatic photoautotrophs is neglected. The uptake of DIC by aquatic photoautotrophs may reach 0.2 to 0.7 Pg C/a globally, indicating that the carbon sink by the coupled carbonate weathering with aquatic photosynthesis mechanism (CCW) may be an important control in climate change. In order to understand the sensitivity of the CCW carbon sink to changes of climate and land-use, a systematic study of modern trap and 100-year-long core sediments was conducted in Fuxian Lake, (Yunnan, SW China), the second-deepest plateau oligotrophic freshwater lake in China. It was found that (1) the autochthonous OC in the lake sediments was characterized by lower C/N ratios and higher $\delta^{13}C_{org}$. By means of an n-alkanes compound calculation, the proportions of autochthonous OC were determined to be in the range, 60–68% of all OC; (2) increase in the autochthonous OC accumulation rate ($OCAR_{auto}$) was accompanied by an increase in the inorganic carbon accumulation rate (ICAR) in both the trap and core sediments. In particular, the post-1950 $OCAR_{auto}$ was estimated to be about 6.9 times that for the period, 1910–1950; (3) $OCAR_{auto}$ in core sediments increased significantly with global warming and land-use change, from 1.06 g C m^{-2} yr^{-1} in 1910 to 21.74 g C m^{-2} yr^{-1} in 2017. The increasing carbon sink may act as a negative feedback on global warming if the trend holds for all lakes globally. This study is the first to quantify the burial flux of organic carbon generated by the BCP effect in lakes and may contribute to solving the problem of the missing carbon sink in the global carbon cycle.

* Corresponding author at: State Key Laboratory of Environmental Geochemistry, Institute of Geochemistry, CAS, Guiyang 550081, Guizhou, China
E-mail address: liuzaihua@vip.gyig.ac.cn (Z. Liu).

https://doi.org/10.1016/j.scitotenv.2020.137539
0048-9697/

1. Introduction

Atmospheric CO_2 concentration has increased from 295 ppm before the Industrial Revolution to 409 ppm in 2018 (www.esrl.noaa.gov/gmd/ccgg/trends/). A critical issue in the study of global climate change is the imbalance in the calculation of atmospheric CO_2 (Broecker et al., 1979; Ciais et al., 2013; Schindler, 1999; Sundquist, 1993; Tans et al., 1990). Recent studies have suggested that the residual terrestrial carbon sink is 2.5–2.8 Pg C/a (Ciais et al., 2013; Melnikov and O'Neill, 2006). According to Regnier et al. (2013), the carbon sink from the global plant-soil system was about 0.9–1.5 Pg C/a. Therefore, there were still about 1–1.5 Pg C/a unaccounted for in the terrestrial ecosystem.

Other studies (Liu et al., 2010, 2011, 2018) show that the carbon sink from the weathering of carbonate minerals, often coupled with aquatic photosynthesis (the biological carbon pump effect – 'BCP'), may be an important contributor to the missing global carbon. Carbonate weathering coupled with aquatic photosynthesis forms organic matter via the reaction (Liu et al., 2010, 2011, 2018):

$$CaCO_3 + CO_2 + H_2O \rightarrow Ca^{2+} + 2HCO_3^- \xrightarrow{\text{photosynth.}} CaCO_3 + x(CO_2 + H_2O) + (1-x)(CH_2O + O_2) \quad (1)$$

where x and 1-x are stoichiometric coefficients.

This challenges the traditional view that only the chemical weathering of silicate minerals in rocks might potentially contribute to or control long-term climate change (Berner, 2003; Li and Elderfield, 2013; Walker et al., 1981). Carbonate weathering rates are several orders of magnitude faster than those of silicates (Beaulieu et al., 2012; Dreybrodt, 1988; White and Brantley, 2003; Zeng et al., 2019b). With the biological carbon pump effect, in which there is aquatic photosynthetic uptake of carbonate weathering-derived DIC and burial of some of the resulting (autochthonous) organic carbon (OC) (Chen et al., 2017; Einsele et al., 2001; Lerman and Mackenzie, 2005; Liu et al., 2015; Maavara et al., 2017; Nõges et al., 2016; Ternon et al., 2000; Yang et al., 2016), the carbon sink via coupled carbonate weathering may be an important contributor to both short-term and long-term climate change (Liu et al., 2010, 2011, 2018).

How does OC generated by the BCP effect respond to climate and land-use changes? and, further, how much of the OC generated by the BCP effect (autochthonous OC) can be buried effectively? (i.e. is no longer available to the atmosphere). Here, differentiating between autochthonous and allochthonous OC is an important first step. Allochthonous OC represents terrigenous sources such as vascular plant tissues, detritus from marshes and upland sources, etc. (Bianchi, 2007; O'Reilly et al., 2014). Traditional geochemical methods (C/N, $\delta^{13}C_{org}$) have generally been used to determine the sources of organic matter in sediments (Chen et al., 2002; Meyers and Ishiwatari, 1993; Ramaswamy et al., 2008; Tue et al., 2011). However, it will be emphasized below that the carbon n-alkane numerical distribution is also important (Huang et al., 2017; Meyers, 2003; Ortiz et al., 2011; Sikes et al., 2009; Silva et al., 2012; Wang and Liu, 2012; Guo, 2016) because, compared to other types of organic components in sediment, n-alkanes contain carbon bonds with high bond energy, i.e. are relatively stable (Blumer et al., 1971; Fokin et al., 2012). While accumulating, the n-alkanes are sensitive to climate and environmental changes, but afterwards are readily preserved in sediments and difficult to degrade (Eglinton and Hamilton, 1967; Meyers, 2003; Schefuß et al., 2003; Volkman et al., 1980).

Lakes can be ideal locations for the preservation of autochthonous OC. Researchers have found that terrestrial lakes and reservoirs have significant potential as carbon sinks in the global carbon cycle (Anderson et al., 2013, 2014; Battin et al., 2009; Buffam et al., 2011; Clow et al., 2015; Cole et al., 2007; Dean and Gorham, 1998; Dietz et al., 2015; Dong et al., 2012; Downing et al., 2008; Einsele et al., 2001; Gui et al., 2013; Heathcote and Downing, 2012; Heathcote et al., 2015; Huang et al., 2017, 2018; Kastowski et al., 2011; Mendonça et al., 2016, 2017; Nõges et al., 2016; Tranvik et al., 2009; Yu et al., 2015; Zhang et al., 2017, 2018). OC burial in lacustrine sediments is characterized by comparatively rapid accumulation (Dean and Gorham, 1998; Cole et al., 2007; Mendonça et al., 2016) and a high preservation factor that on average is 50 times greater than that observed in the oceans (Einsele et al., 2001).

The aim of this study is to better understand the sensitivity of the carbon sink by the coupled carbonate weathering-BCP effect to climate and land-use changes. A systematic study of trap and core sediments was conducted in Fuxian Lake, the second-deepest plateau oligotrophic freshwater lake in Southwest China. Sediment core was used to know the past change in the carbon sink by coupled carbonate weathering, while the modern trap was used to reveal sensitivity of the carbon sink to climate and land-use changes in more details. We try: 1) to distinguish autochthonous and allochthonous sources of OC in the lake sediment; 2) to quantify the extent to which the autochthonous OC accumulation rate (OCAR) has changed over the past century; 3) to examine the relationships between autochthonous OCAR and the climate and/or land-use changes.

2. Site description

Fuxian Lake (24°17′–24°37′N, 102°49′–102°57′E) is located at 1722.5 m a.s.l. on a plateau in central Yunnan Province, Southwest China (Fig. 1). As the second deepest freshwater lake in China (158 m), with a large volume (20.62 billion m^3) and water surface area (212 km^2), and yet a small catchment area (675 km^2), water in the lake has the unusually long mean residence time of 167 years (Wang and Dou, 1998). The hydrochemical type is HCO_3^--Ca-Mg, which is typical of limestone karst water. It is an oligotrophic lake, one of the most crucial freshwater resources in China. The lake basin is wide and deep in the north, narrow and comparatively shallow in the south (Fig. 1). The lake receives the flow from more than twenty short streams (e.g., Liangwang River, Dongda River), and has the Haikou River as its single outlet (Liu et al., 2009). The average annual temperature of the Fuxian Lake basin is 15.6 °C, and annual average precipitation is 951 mm. The dry season and the rainy season are clearly demarcated, 83% of precipitation being concentrated in the rainy season from May to October.

3. Methods

3.1. Sampling the lake sediments

Three moorings with sediment traps were positioned in the center of the lake (depth of water about 120 m at site FX-2, Fig. 1), and were fastened to an iron buoy on Jan. 15, 2017. The traps were open-topped cylindrical polyethylene tubes (105 cm in length, with an inner diameter of 15 cm). They were set at water depths of 40 m, 80 m, 110 m, and emptied quarterly over the study year, 2017. The material collected was transferred into plastic containers in the field and stored at 4 °C prior to sub-sampling. The sediments were freeze-dried to constant weight and homogenized, in preparation for elemental analysis.

Three sediment cores were collected on January 20 2017 from the northern (FX-1), central (FX-2) and southern (FX-3) sectors of the lake (Fig. 1), using a gravity corer fitted with 58-mm internal diameter perspex tubes. The cores (15–20 cm long) were sectioned into 1 cm intervals, transported to the laboratory in pre-cleaned polyethylene bags immediately after collection, and then freeze-dried.

3.2. Dating the core sediments

For radiometric dating, the freeze-dried and homogenized core sediments were cut into 1 cm intervals. Activities of ^{210}Pb and ^{226}Ra were

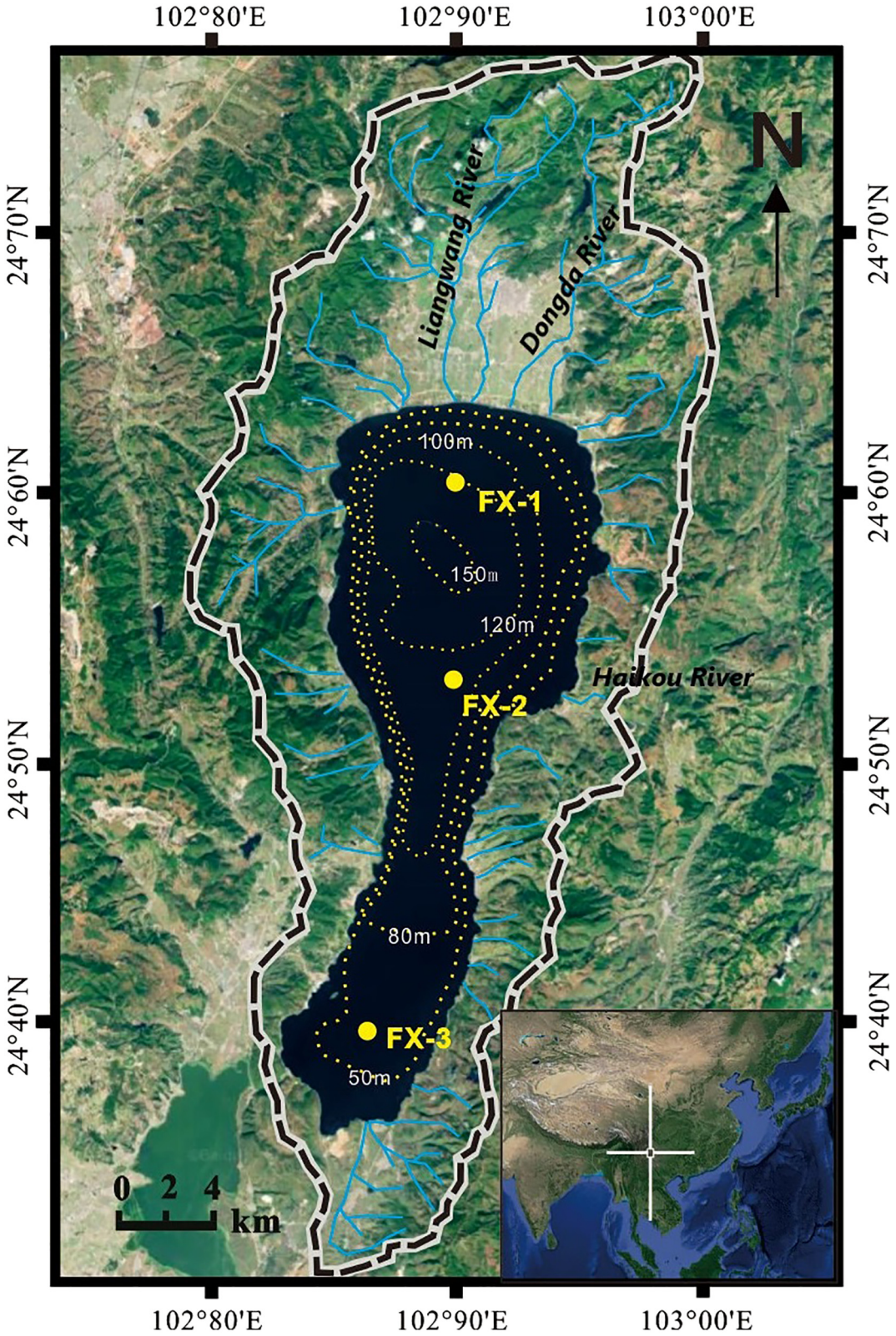

Fig. 1. Location of Fuxian Lake and the sampling sites. FX-1, FX-2 and FX-3 are sediment core sites representing the northern, central and southern sectors of the Lake, respectively. The basin boundary (black dashed line) and lake depth contours (dotted lines) are from Liu et al. (2008).

measured with a large volume, coaxial Reversed Electrode High-Purity Germanium detector (Canberra; >60% relative efficiency), following Kirchner and Ehlers (1998). The weighed sediment samples (10 g) were placed in capped plastic test tubes for three weeks of sealed storage to ensure decay to radioactive equilibrium. The activity excess ^{210}Pb ($^{210}Pb_{ex}$) was obtained by subtracting the activity of ^{226}Ra from that of total ^{210}Pb (Appleby, 2002). The constant rate of supply (CRS) model, $^{210}Pb_{ex}$, was used to date the sediment (Appleby, 2002, 2008;

Sanchez-Cabeza and Ruiz-Fernández, 2012):

$$t = \frac{1}{\lambda} \ln\left(\frac{A_n}{A_0}\right) \quad (2)$$

where t is the age in years, λ is the decay constant of ^{210}Pb (0.03114 yr^{-1}), A_n is the content of $^{210}Pb_{ex}$ at each sediment depth, and A_0 is the total content of ^{210}Pb in the sediment core.

3.3. Measurement of organic carbon, inorganic carbon and TOC/TN

Total carbon (TC) was determined by elemental analyzer (Elementar-vario MACRO cube). Total organic carbon (TOC) content, total nitrogen (TN) content, and TOC/TN (atomic) ratios were determined on the sediments, following acid treatment with 1.5 mol/L HCl for 24 h to remove inorganic carbon. The carbonate-free samples were triple-rinsed with distilled water to remove acid residues, and dried at 60 °C for 48 h. The MACRO analyzer which was calibrated with sediment standard materials (B2150 and AR2026) for a typical measurement precision of 0.2%. The inorganic carbon (IC) content was then calculated as the difference between TC and TOC. The accumulation rates of organic carbon (OCAR) and inorganic carbon (ICAR) (g C m^{-2} yr^{-1}) were estimated by

$$\text{OCAR (or ICAR)} = \frac{\partial Md}{\partial t} = \frac{\rho * \partial Z/\partial t}{\partial t} * C \quad (3)$$

where Md is the mass depth (g cm^{-2}), t is time (years), Z is depth (cm), ρ is the dry bulk density (g cm^{-3}) and C is the concentration of organic carbon and inorganic carbon (mg g^{-1}).

3.4. Measurement of stable carbon isotope ratios

The stable carbon isotope ratios ($\delta^{13}C$) of organic carbon and inorganic carbon in the samples were analyzed by MAT-252/253 mass spectrometer. The results are reported as per mil relative to the international standard, Vienna Peedee Belemnite (VPDB). The instrument analytical precision is better than ±0.03‰ (Sun et al., 2011). $\delta^{13}C$ is calculated as: $\delta^{13}C_{sample} = (R_{sample}/R_{standard}\text{-}1) \times 1000$. In this equation, R is the $^{13}C/^{12}C$ ratio of the sample.

3.5. N-alkane extraction and analysis

Sediment samples for lipid determination were first Soxhlet-extracted from bulk samples (3 g) using dichloromethane–methanol mixture (93:7 v:v), to obtain the soluble fraction. The samples were re-extracted by n-hexane, and the combined organic phase set over anhydrous Na_2SO_4 overnight to reduce traces of water. A portion of the extract was saponified (70 °C for 2 h) using KOH-MeOH solute mixture (3 mL). n-alkanes were then extracted into n-hexane from the saponified sample and concentrated to 1 mL using rote-evaporation (Waterson and Canuel, 2008). N-alkanes were quantified by measuring the concentrated eluent by gas chromatography (GC) with an Agilent 7890A instrument. The GC procedures were as follows: For n-alkanes, temperature was raised from 70 °C (held for 1 min) to 140 °C at 10 °C/min, and then at 3 °C/min to 310 °C (held for 15 min) (Mortillaro et al., 2011).

3.6. Calculation of OCAR from autochthonous and allochthonous sources

Previous studies have revealed that organic matter C/N ratio values, $\delta^{13}C$, and $\Delta^{14}C$ can be used to indicate the relative contribution of allochthonous versus autochthonous organic matter to lake sediments (Chen et al., 2002; Meyers and Ishiwatari, 1993; Ramaswamy et al., 2008; Tue et al., 2011; Chen et al., 2017). However, each method has its limitations in practical application. At present, there is no recognized reliable method to quantitatively distinguish the sources of organic carbon. This research method (n-alkanes) will be a useful exploration for quantitative organic carbon sources method.

Compared to traditional geochemical methods ($\delta^{13}C_{org}$, C/N), biomarker compounds (n-alkanes) in lake sediments are now widely used as tracers (or proxies) to characterize the sources of organic matter due to their source specificity and higher resistance to bacterial degradation (Blumer et al., 1971; Eglinton and Hamilton, 1967; Fokin et al., 2012; Meyers, 2003; Schefuß et al., 2003; Volkman et al., 1980). In general, many aquatic algae and bacteria are dominated by short-chain n-alkanes normally represented by nC15, nC17 and nC19 (Bourbonniere and Meyers, 1996; Canuel et al., 1997; Giger et al., 1980; Meyers, 2003) with unimodal distribution maximizing. A unimodal distribution maximizing at nC17 indicates algae and photosynthetic bacteria sources (Meyers, 1997, 2003). Submerged and floating aquatic plants commonly maximize n-alkanes at mid-chain numbers, normally by nC21, nC23 and nC25 (Ficken et al., 2000; Meyers, 2003; Ogura et al., 1990; Viso et al., 1993), while the abundance of long-chain n-alkanes (normally represented by nC27, nC29 and nC31) has been used extensively as an indicator of terrestrial sources of origin (Bourbonniere and Meyers, 1996; Eglinton and Hamilton, 1967; Meyers, 1997, 2003; Rao et al., 2014). Organic carbon in the Fuxian Lake sediments included both autochthonous and allochthonous OC. The allochthonous OC was derived from long-chain n-alkanes (nC27, nC29 and nC31). We interpreted short-chain n-alkanes (nC15, nC17 and nC19) and mid-chain n-alkanes (nC21, nC23 and nC25) as autochthonous OC. Simple End-member Modeling can then undertaken by:

$$R_{auto} = \frac{\sum(nC15 + nC17 + nC19) + \sum(nC21 + nC23 + nC25)}{\sum(nC15 + nC17 + nC19) + \sum(nC21 + nC23 + nC25) + \sum(nC27 + nC29 + nC31)} \quad (4)$$

where R_{auto} is the proportion of autochthonous OC. Correspondingly, $R_{allo} = 1\text{-}R_{auto}$, is the proportion of allochthonous OC (Guo, 2016).

The organic carbon accumulation rates from autochthonous and allochthonous sources can then be derived:

$$OCAR_{auto} \text{ (or } OCAR_{allo}) = OCAR \times R_{auto} \text{ (or } R_{allo}) \quad (5)$$

where OCARauto and OCARallo are the organic carbon accumulation rates from autochthonous and allochthonous OC, respectively.

4. Results

4.1. Distribution of $^{210}Pb_{ex}$ and dating results

The vertical distribution of $^{210}Pb_{ex}$ specific activity in cores FX-1, FX-2 and FX-3 generally displayed exponential decreases with depth when they were plotted against cumulative mass (Fig. 2), which ranged from 32.78 ± 12.99 to 397.62 ± 40.08 Bq kg^{-1}, with a mean value of 105.81 ± 20.34 Bq kg^{-1}. The exponential decreases were similar to profiles observed in previous studies (Liu et al., 2009; Li et al., 2011; Liu et al., 2013; Wang et al., 2018), indicating that $^{210}Pb_{ex}$ CRS model was suitable for dating the sediments of Fuxian Lake. As calculated by the $^{210}Pb_{ex}$ CRS model the period covered by each core was about 100 years, from ~1910 to 2017, as shown in Fig. 2.

4.2. C and N contents and accumulation rates in the trap and core sediments

The material collected from the sediment traps revealed that there were important changes during the year of sampling. Total accumulation rates (Total AR) showed an obvious seasonal variation, with lower values (0.44–0.70 g C $m^{-2}d^{-1}$) mainly during spring and winter and the higher values (1.00–2.95 g C $m^{-2}d^{-1}$) during summer and fall (Table 1). There were higher values

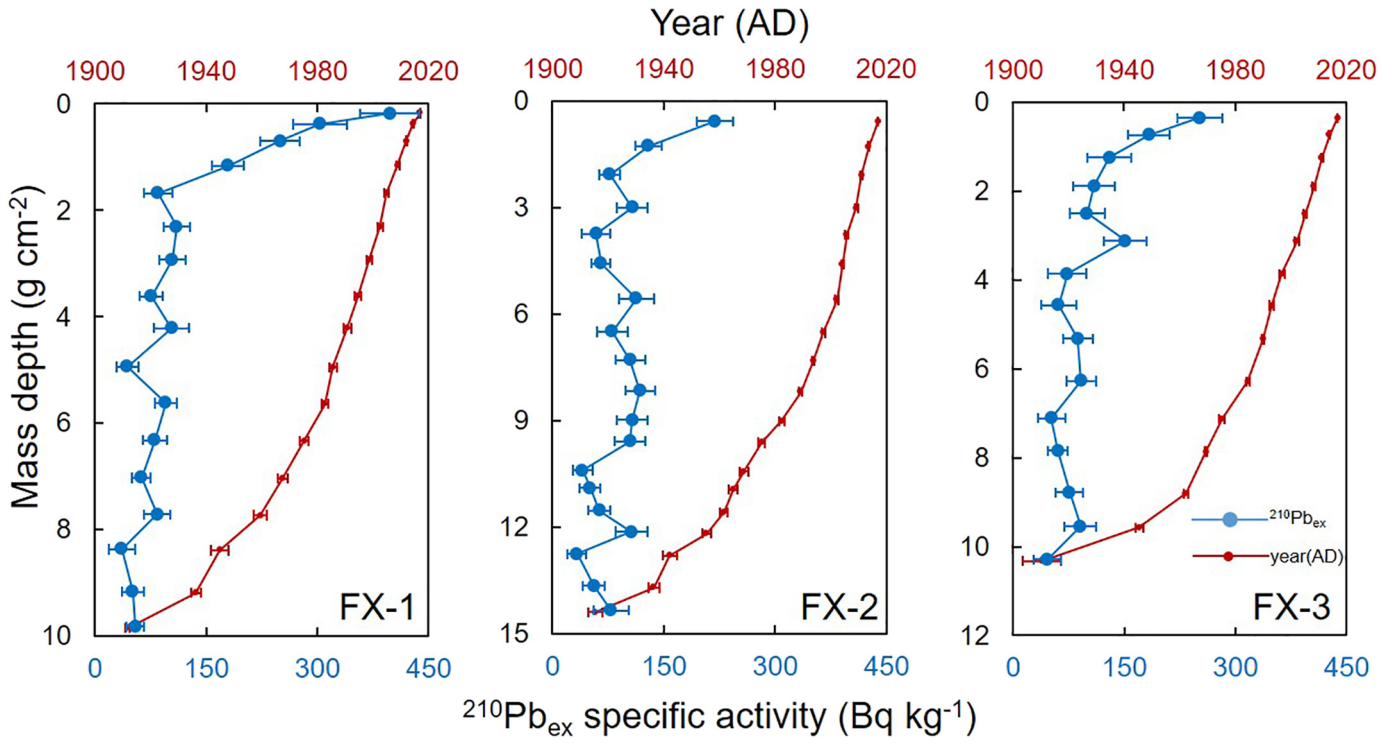

Fig. 2. Vertical profiles of $^{210}Pb_{ex}$ in sediment cores FX-1, FX-2 and FX-3, Fuxian Lake. The geochronology of the sediment cores was estimated from the $^{210}Pb_{ex}$ CRS model and ^{137}Cs.

(92.21–107.78 mg g^{-1}) of TOC in the winter and spring and higher TIC (63.54–80.83 mg g^{-1}) in the summer and fall. Increased inorganic carbon accumulation rates (ICAR) were roughly matched by increased organic carbon accumulation rates (OCAR), with both reaching their highest values in summer and fall (ICAR: 0.07–0.24 g C $m^{-2}d^{-1}$; OCAR: 0.08–0.13 g C $m^{-2}d^{-1}$) (Table 1). The C/N ratio is a frequently-used index feature in sediments, but there were no obvious seasonal changes here (Table 1).

While the core sediments from all three sites displayed simple exponential decreases of TOC with depth, average TOC values were significantly higher at FX-1 (23.42 mg g^{-1}) than at the other two sites (FX-2, 15.02 mg g^{-1}; FX-3, 12.41 mg g^{-1}; Table 2). TOC content in FX-1, FX-2 and FX-3 ranged from 8.75 to 31.22 mg g^{-1}, 6.23 to 18.22 mg g^{-1} and 4.54 to 23.07 mg g^{-1}, respectively. The TIC content at FX-1, FX-2 and FX-3 also showed exponential decreases with depth, ranging 3.43–18.79 mg g^{-1}, 11.65–18.92 mg g^{-1} and 12.83–24.88 mg g^{-1}, respectively. Positive correlations between TOC and TIC were apparent at each site (FX-1: $R^2 = 0.81$, $P < 0.0001$, $n = 17$; FX-2: $R^2 = 0.56$, $P < 0.0003$, $n = 19$; FX-3: $R^2 = 0.40$, $P < 0.02$, $n = 15$). Meanwhile, the C/N ratios were essentially lower than 10, with a tendency to decrease from the surface to the bottom (Fig. 3, Table 2).

From the base to the top, OCARs at FX-1, FX-2 and FX-3 ranged from 2.35 to 36.44 g C m^{-2} yr^{-1}, 2.33 to 41.64 g C m^{-2} yr^{-1}, and 1.06 to 26.28 g C m^{-2} yr^{-1}, respectively (Table 2). Base to top ICARs at FX-1, FX-2 and FX-3 similarly ranged 1.19 to 25.74 g C m^{-2} yr^{-1}, 4.55 to 83.07 g C m^{-2} yr^{-1}, and 2.72 to 48.89 g C m^{-2} yr^{-1}, respectively (Table 2).

4.3. Carbon isotope ratios of the organic and inorganic carbon in the trap and core sediments

In the trap sediments, there were positive correlations between $\delta^{13}C_{org}$ (−20.88 to −25.37‰) and $\delta^{13}C_{carb}$ (−0.35–0.007‰), with higher values in summer and fall (Fig. 4). In cores FX-1, FX-2, FX-3, $\delta^{13}C_{org}$ displayed exponential increases with depth, ranging from −28.07 to −24.77‰, −27.71 to −24.87‰, and −27.39 to −24.24‰, respectively (Fig. 3). These patterns followed those of the $\delta^{13}C_{carb}$ records at all three sites, which ranged from −0.67 to −0.31‰, −0.49 to 0.27‰, and 0 to 0.98‰, respectively (Table 2). There was weakly positive correlation between $\delta^{13}C_{org}$ and $\delta^{13}C_{carb}$ in FX-2 ($R^2 = 0.55$) and a stronger relation in FX-3 ($R^2 = 0.82$). In FX-1, there was no clear correlation over the core as a whole ($R^2 = 0.04$, $P < 0.5$, $n = 17$). However, when this profile was cut into two parts (0–4 cm, 4–17 cm), the correlation

Table 1
Dry weight, TOC and TIC contents, C/N ratios, $\delta^{13}C_{carb}$, $\delta^{13}C_{org}$, OCAR, ICAR and Total AR determined by sediment traps at site FX-2, Fuxian Lake, from different water depths in different seasons.

Season	Water depth (m)	Dry weight (g)	TOC (mg g^{-1})	TIC (mg g^{-1})	C/N	$\delta^{13}C_{carb}$ (‰)	$\delta^{13}C_{org}$ (‰)	OCAR (g C $m^{-2}d^{-1}$)	ICAR (g C $m^{-2}d^{-1}$)	Total AR (g C $m^{-2}d^{-1}$)
Spring (Jan. 15–Apr. 16)	40	0.71	106.57	3.22	9.44	−1.31	−26.98	0.047	0.001	0.442
	80	1.01	92.45	6.63	9.49	−0.68	−26.37	0.058	0.004	0.628
	110	1.13	107.78	9.14	8.60	−1.40	−27.27	0.076	0.006	0.703
Summer (Apr. 16–July 16)	40	1.61	76.48	72.82	9.30	−0.35	−24.63	0.077	0.073	1.001
	80	2.07	66.41	73.79	10.17	−0.29	−24.48	0.085	0.095	1.287
	110	1.87	80.97	63.54	10.18	−0.16	−25.37	0.094	0.074	1.163
Fall (July 16–Oct. 15)	80	4.74	45.20	80.87	6.65	0.01	−20.88	0.133	0.238	2.947
Winter (Oct. 15–Jan. 14)	40	0.77	102.24	18.39	7.06	−0.85	−23.89	0.049	0.009	0.479
	110	0.77	92.21	17.07	8.38	−0.68	−23.52	0.044	0.001	0.481

Table 2
TOC and TIC contents, C/N ratios, $\delta^{13}C_{carb}$, $\delta^{13}C_{org}$, OCAR and ICAR of the core sediments of Fuxian Lake.

Site	TOC (mg g^{-1})	TIC (mg g^{-1})	C/N	$\delta^{13}C_{carb}$ (‰)	$\delta^{13}C_{org}$ (‰)	OCAR (g C m^{-2} yr^{-1})	ICAR (g C m^{-2} yr^{-1})
FX-1	8.75–31.22[a]	3.43–18.79	7.54–10.71	−0.67 to −0.31	−28.07 to −24.77	2.35–36.44	1.19–25.74
	(13.78)[b] [1.83][c]	(7.93) [0.98]	(8.76) [0.24]	(−0.47) [0.02]	(−26.13) [0.26]	(16.68) [2.25]	(10.33) [1.55]
FX-2	6.23–18.22	11.65–18.92	7.53–9.89	−0.49–0.27	−27.71 to −24.87	2.33–41.64	4.55–83.07
	(7.92) [0.62]	(14.25) [0.53]	(8.14) [0.14]	(0.00) [0.05]	(−25.60) [0.15]	(16.98) [2.73]	(31.03) [5.14]
FX-3	4.54–23.07	12.83–24.88	5.80–7.74	0–0.98	−27.39 to −24.24	1.06–26.28	2.72–48.89
	(8.27) [1.20]	(19.55) [0.85]	(6.64) [0.18]	(0.52) [0.08]	(−25.75) [0.20]	(12.38) [1.83]	(29.78) [3.49]

[a] Minimum-maximum.
[b] Mean values.
[c] Standard error.

coefficients (R^2) improved to 0.66 and 0.55 respectively, indicating that there had been a significant change in recent depositional conditions (Fig. 4).

4.4. Distribution of n-alkanes and proportions of autochthonous carbon

In the samples, the n-alkane distributions ranged from nC12 to nC34. The total concentrations of n-alkanes ($\sum$(nC10 to nC34)) ranged from 8929 ng g^{-1} to 51,973 ng g^{-1}, with a mean value of 20,161 ng g^{-1}. The overall pattern was of mainly short-chain n-alkanes. The n-alkanes displayed a bimodal carbon number distribution with little odd-even imbalance within the high carbon numbers (nC25 to nC33). The relative abundances of short-chain n-alkanes (below nC20) were higher, chiefly nC17 (349 ng/L to 8846 ng/L; average, 1898 ng/L), nC18 (333 ng/L to 7230 ng/L; average, 1673 ng/L) as the peak carbon numbers, with no evident predominance of odd or even. The values of various indices in the sediments are shown in Table 3. In the Carbon Preference Index (CPI), CPI1 varied between 0.78 and 1.12 (average = 0.93). CPI2 values varied between 0.82 and 1.44 (average = 1.06; Table 3). The n-alkane ACL index (Average Chain Length) is the concentration-weighted mean chain length of n-alkanes present in a geological sample. Its value ranged between 29.08 and 30.48, with an average of 29.57 (Table 3). The *P*aq index represents the proportion of non-emergent aquatic plant matter in the lake sediments compared to that of the emergent aquatic and the terrestrial plants (Ficken et al., 2000; Zhang et al., 2004; Zheng et al., 2007). *P*aq values in Fuxian Lake sediment samples varied between 0.18 and 0.48, with a mean of 0.39 (Table 3). OEP (Odd Even Preference) reflects the maturity of organic matter. OEP values in Fuxian Lake sediment samples varied between 0.26 and 1.38, with a mean value of 0.78 (Table 3).

In addition, the calculated average proportions of autochthonous OC at FX-1, FX-2 and FX-3 were approximately 61%, 68% and 60% of the total OC, respectively (Table 3). The $OCAR_{auto}$ at FX-1, FX-2 and FX-3 displayed increases with time, especially after the 1950s and again after 1980s and 2000s, ranging from 1.13 to 19.88 g C m^{-2} yr^{-1}, 1.43 to 29.01 g C m^{-2} yr^{-1}, and 0.61 to 16.33 g C m^{-2} yr^{-1}, respectively (Fig. 5, Table 2).

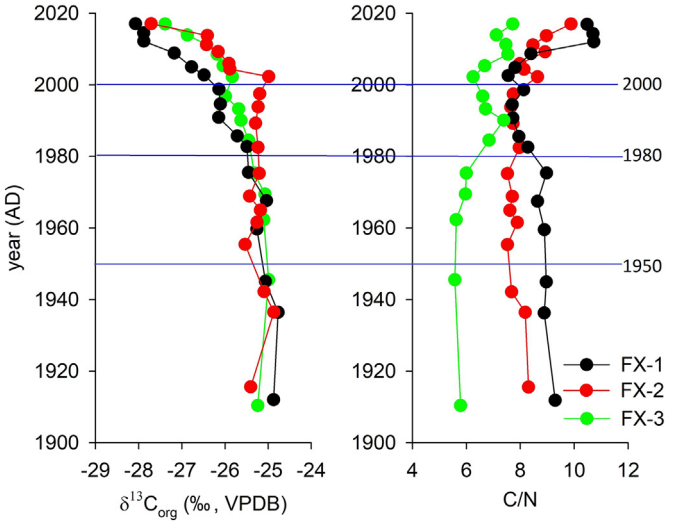

Fig. 3. Temporal sequences of $\delta^{13}C_{org}$ and C/N in cores FX-1, FX-2 and FX-3, Fuxian Lake. Note the large changes at around the years 1950, 1980 and 2000.

5. Discussion

5.1. Changes in the autochthonous sources of OC in sediments of Fuxian Lake

5.1.1. Distribution characteristics of C/N and $\delta^{13}C_{org}$

The trend of C/N ratios in the core sediments was in sharp contrast to the effect of diagenesis on organic matter composition. Because nitrogen compounds are usually preferentially re-mineralized, C/N ratios are expected to increase with diagenesis and depth in a core (Meyers, 1997). The decreasing trend in the Fuxian C/N ratios with depth, therefore, may indicate that alternation of the sources of the organic matter prevailed over diagenesis.

C/N ratios from all terrestrial foliage in the Fuxian Lake basin were in the range, 24.45 to 25.03 (Fig. 6). Generally, terrestrial plants and emergent macrophytes are rich in fiber but low in proteins, and therefore their C/N ratios are larger than 20 (Meyers, 2003). Lake algae and plankton contain low amounts of fiber but more proteins, and their C/N ratios are generally <10 (Meyers, 2003). Tyson (2012) listed specific C/N ratios for a range of organic matter. Plankton have average C/N ratios of ~6, with most diatoms varying between 5 and 8. Freshwater macrophytes have C/N ratios of 12 or more. In our study, the submerged plants in Fuxian Lake had a C/N ratio of 9.92 (Fig. 6). A previous study (Chen et al., 2015) found that lake productivity was positively correlated to species richness in this lake, and that biomass composition showed an elevated proportion of benthic species relative to phytoplankton since the 1950s. As shown in Fig. 6, the C/N ratios of both core and trap sediments fell within the field of autochthonous organic matter (aquatic plants), and are clearly different from the field of allochthonous organic matter (terrestrial plants). An interesting finding is that C/N ratios in the core sediments increased by 1.94–3.17 from the 1910s to present, which is similar to the results of simulation experiments that obtained increases from 6.0 to 8.0 at the Espegrend Marine Biological Station (at Raunefjorden, 60.3°N, 5.2°E) of the University of Bergen, Norway (Riebesell et al., 2007). The reason for this change is that the plankton community consumed more DIC as the partial pressures of CO_2 increased, resulting in higher values of C/N (Riebesell et al., 2007). This process also strengthened the "DIC fertilization effect" (Chen et al., 2017; Yang et al., 2016; Zeng et al., 2019a) and increased the autochthonous sources of OC (i.e., increasing ratios of autochthonous carbon in Fig. 5).

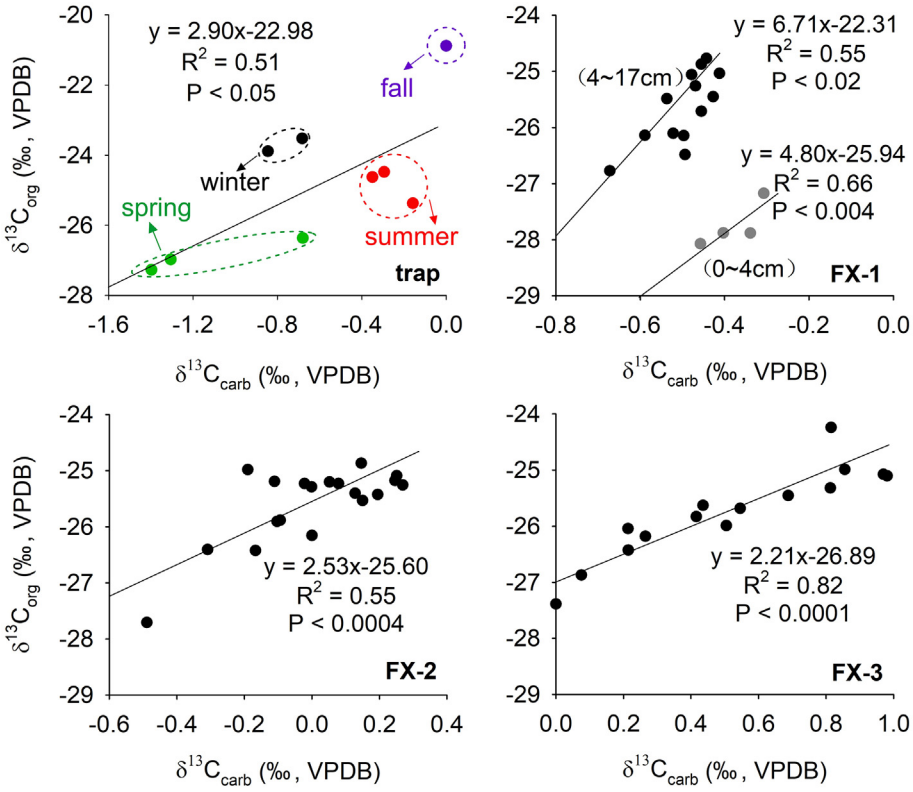

Fig. 4. Correlations between $\delta^{13}C_{org}$ and $\delta^{13}C_{carb}$ in the trap sediments (during the monitoring period 1/2017–1/2018), and within cores FX-1, FX-2, FX-3, Fuxian Lake. FX-1 was divided into two sections (0 to −4 cm, −4 to −17 cm).

$\delta^{13}C_{org}$ values exhibited a decreasing trend from 1910 to the present (Fig. 3), similar to those measured in a previous study in Fuxian Lake (Zhang et al., 2015). The reason for this decrease may be a combination of (1) enhanced aquatic photosynthesis, which brought more negative $\delta^{13}C$ into the organic matter by isotopic fractionation (Falkowski and Raven, 1997); (2) expansion of the chemoautotrophic microbial communities with intensified eutrophication, introducing greater fractionation effects than those associated with photosynthesis (Kelley et al., 1998); (3) increased input of terrestrial C3 plants, bringing more negative $\delta^{13}C_{org}$ (average, −27‰) organic matter (Meyers, 1994); (4) increased degradation of organic matter, which produces more $^{12}CO_2$ that is gradually consumed by algae, resulting in a more negative $\delta^{13}C_{org}$ in the organic matter (Chen et al., 2018); (5) the depletion in atmospheric $\delta^{13}CO_2$, which has been declining at an increasing rate during the past 200 years due to deforestation and the burning of fossil fuels (Verburg, 2007). In addition, there was a positive relationship between $\delta^{13}C_{org}$ and $\delta^{13}C_{carb}$ ($R^2 = 0.51$, $P < 0.05$, $n = 9$) in the trap sediments during the sample year, and regression analysis also showed significant correlations between $\delta^{13}C_{org}$ and $\delta^{13}C_{carb}$ in the core sediments (Fig. 4). Meyer et al. (2013) believed that positive relationships between $\delta^{13}C_{org}$ and $\delta^{13}C_{carb}$ suggested that both the inorganic and organic carbon records reflect variation in the isotopic composition of contemporaneous DIC. Therefore, these observations may confirm that the source of the sedimentary OC in Fuxian Lake was mainly autochthonous OC, i.e., organic carbon burial by the BCP effect may play a significant role in the carbon cycle there.

As noted, core FX-1 was divided into two sections (0–4 cm and >4–17 cm) because $\delta^{13}C_{org}$ values decreased abruptly to <−27‰ at the 4 cm mark and then continued to decline rather steadily to −28‰ at the top (0 cm). This was probably caused by an abruptly increased input of allochthonous materials due to soil erosion that resulted from widespread exploitation of the land since 2009, enhancing input of

Table 3
Mean value of proxies of n-alkanes and proportion of autochthonous and allochthonous sources of OC in the core sediments at Fuxian Lake.

Site	CPI1	CPI2	ACL	Paq	OEP	R_{auto} (%)	R_{allo} (%)
FX-1	0.90–1.12[a] (0.95)[b] [0.02][c]	0.92–1.44 (1.10) [0.04]	29.17–29.94 (29.57) [0.08]	0.27–0.48 (0.39) [0.02]	0.75–1.38 (0.93) [0.06]	47.55–70.97 (60.85) [0.03]	29.03–52.45 (39.15) [0.03]
FX-2	0.92–1.06 (0.95) [0.01]	1.02–1.12 (1.07) [0.01]	29.08–29.77 (29.52) [0.08]	0.41–0.48 (0.44) [0.01]	0.72–1.23 (0.87) [0.05]	61.37–83.82 (68.48) [0.03]	16.18–38.63 (31.52) [0.03]
FX-3	0.77–1.00 (0.89) [0.02]	0.82–1.33 (1.00) [0.04]	29.18–30.48 (29.62) [0.11]	0.18–0.44 (0.33) [0.03]	0.26–0.88 (0.55) [0.06]	46.86–71.27 (59.83) [0.02]	28.73–53.14 (40.17) [0.02]
Mean	0.93	1.06	29.57	0.39	0.78	63.05	36.95

CPI1 = ∑odd(nC15-nC34)/∑even(nC15-nC34); CPI2 = 1/2((nC25 + nC27 + nC29 + nC31 + nC33)/(nC24 + nC26 + nC28 + nC30 + nC32) + (nC25 + nC27+ nC29 + nC31 + nC33)/(nC26 + nC28 + nC30 + nC32 + nC34)); ACL = [25(nC25) + 27(nC27) + 29(nC29) + 31(nC31) + 33(nC33)]/(nC25 + nC27 + nC29+ nC31 + nC33); Paq = (nC23 + nC25)/(nC23 + nC25 + nC29 + nC31); OEP = (nC25 + 6nC27 + nC29)/(4nC26 + 4nC28) (Jeng, 2006; Sojinu et al., 2010; Ortiz et al., 2011). R_{auto} is the proportion of autochthonous OC, calculated by End-member Modeling (Eq. (2), see text for details); R_{allo} (the proportion of allochthonous OC) = 1-R_{auto}.

[a] Minimum-maximum.
[b] Mean values.
[c] standard error.

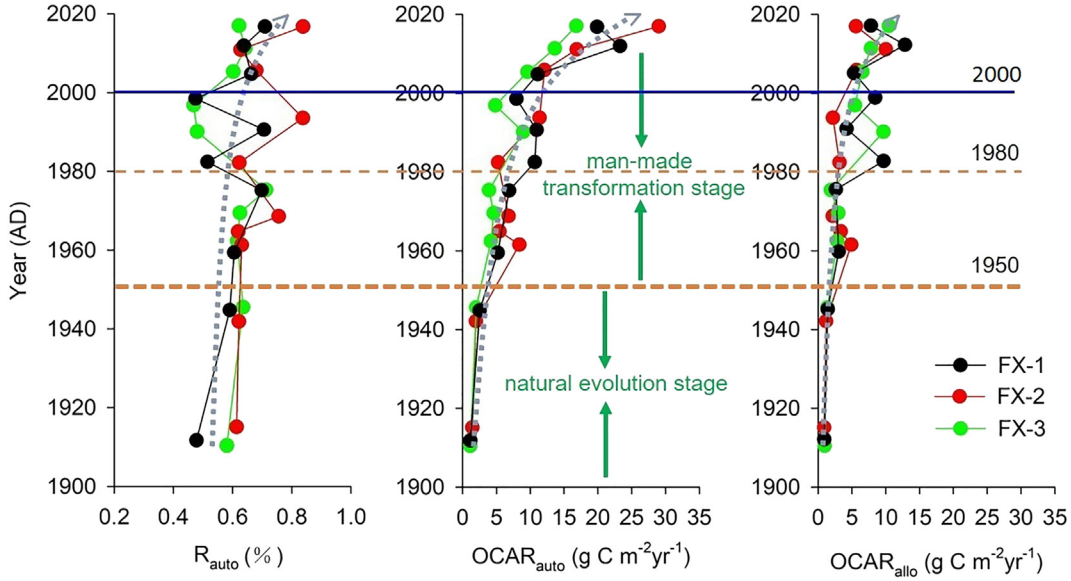

Fig. 5. The temporal sequences of R_{auto} (proportion of autochthonous OC), $OCAR_{auto}$ (accumulation rate of autochthonous OC) and $OCAR_{allo}$ (accumulation rate of allochthonous OC) in cores FX-1, FX-2 and FX-3 in Fuxian Lake. Note the big changes around the years 1950, 1980 and 2000.

allogenic organic matter (^{13}C-depleted), which caused $\delta^{13}C_{org}$ in the sediments to decrease abruptly (Fig. 3).

5.1.2. Source assignments of n-alkanes

The proxies of n-alkanes for each site are shown in Table 3. The high CPI values (>5) indicate more contributions from the epicuticular waxes of vascular plants, whereas low CPI values probably indicate relatively high contributions from the algal and bacterial communities, and/or the aquatic plants (Seki et al., 2006; Tareq et al., 2005; Tolosa et al., 2004). The values of CPI1 and CPI2, with mean values of 0.93 and 1.06, indicate that the n-alkanes had an autochthonous source. The ACL value is greater in higher plants than in lower plants and aquatic algae (Poynter and Eglinton, 1990). The low variation in the ACL of the Fuxian Lake sediments was due to the low input of petrogenic hydrocarbons (Jeng, 2006) (Table 3). With the increase of maturity, n-alkanes gradually lose their specific parity in the course of diagenesis (Meyers and Ishiwatari, 1993; Snedaker et al., 1995). Hydrocarbons composed of a mixture of compounds originating from land plant material show a predominance of odd-numbered carbon chains with OEP of 2–10. OEP values (0.26–1.38) in Fuxian Lake samples indicate that the n-alkanes did not have a strong odd-even preference in higher plants. It is proposed that the high *P*aq value (range 0.1 to 1) corresponds to an increased contribution from aquatic plants, especially submerged and floating plants, and *P*aq < 0.1 corresponds to terrestrial plants (Ficken et al., 2000; Zhang et al., 2004; Zheng et al., 2007). *P*aq values (0.18–0.48) in Fuxian Lake sediments suggest a period relatively

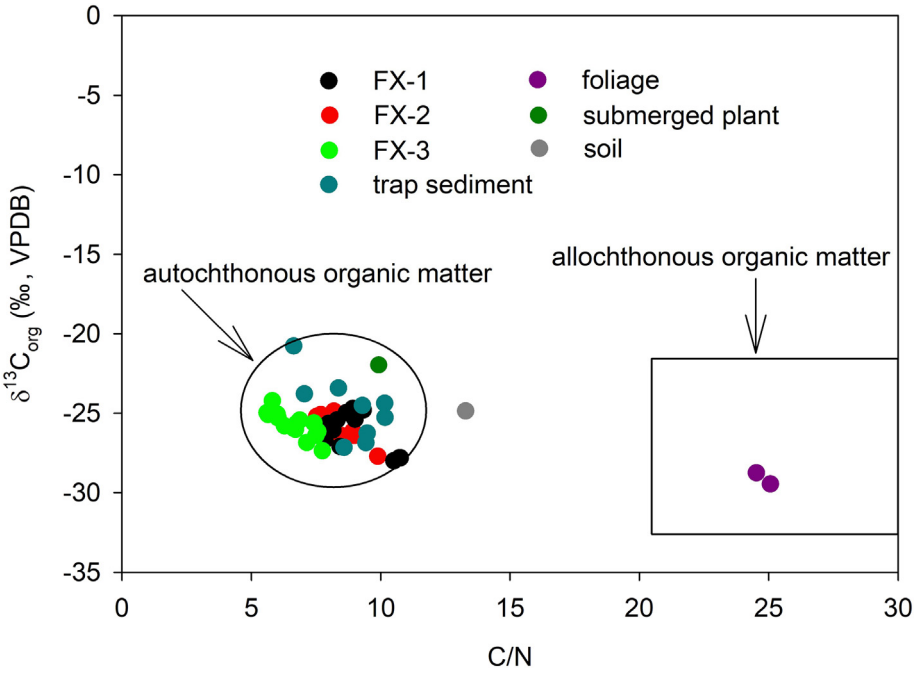

Fig. 6. Distinctive source combinations of C/N ratios and $\delta^{13}C_{org}$ values of the core sediments, trap sediments, soil, foliage and submerged plants in Fuxian Lake (C/N ratios and $\delta^{13}C_{org}$ values for sources of allochthonous and autochthonous are from Meyers (1994)).

enriched in submerged/floating plants and a reduction in emergent/terrestrial plants.

Further, from the biomarker compounds (n-alkanes), the proportions of autochthonous OC ranged 60–68% (Fig. 5), suggesting that autochthonous sources were the chief contributors to the sediments.

5.2. The significant role of organic carbon burial by the BCP effect in lake sediments

5.2.1. Synchronous increase in $OCAR_{auto}$ and ICAR caused by the BCP effect

As shown in Eq. (1), when the BCP effect occurs in aquatic ecosystems, there will be a synchronous increase in $OCAR_{auto}$ and ICAR. Kelts and Hsü (1978) found that the intensity of photosynthesis of aquatic organisms can affect $CaCO_3$ content to some extent. The flourishing of lake aquatic plants leads to large CO_2 uptake in the lake water, which causes carbonate supersaturation over the short term. Therefore, the synchronous increase of $OCAR_{auto}$ and ICAR could be produced by the photosynthesis of aquatic organisms when the latter is strong (Dittrich and Obst, 2004; Kelts and Hsü, 1978). However, $OCAR_{auto}$ and ICAR are found to be in inverse correlation in some lake sediments. Dean (1999) suggested that the decomposition of a higher OC content (>12%) in the sediments will result in a lower pH in the interstitial waters and, therefore, greater dissolution of $CaCO_3$. In the present study, the OC concentration in the sediments was <12% (core sediments: 0.45–3.12%; trap sediments: 9.22–10.78%), suggesting that the effect of decomposition of OC on $CaCO_3$ deposition was small. The seasonal patterns of total accumulation dynamics in Fuxian Lake were strongly coupled with biogeochemical processes. Sediment rates reached maximum values in summer and fall (Table 1, Fig. 7) that matched the maximum phytoplanktonic growth in the lake (Cui et al., 2008). There was a strong correlation between OCAR and ICAR in the trap sediments ($R^2 = 0.86$, $P < 0.0005$, $n = 9$), with values of OCAR higher during summer and fall, the main period of calcite deposition (Fig. 7). Similarly, the core sediment records show that $OCAR_{auto}$ and ICAR were both increasing and displaying significant correlation during the past century (Fig. 7). These observations indicate that the BCP effect was the major mechanism driving the synchronous increases in $OCAR_{auto}$ and ICAR.

5.2.2. Changes in autochthonous and allochthonous organic carbon burial

$OCAR_{auto}$ at FX-1 and FX-2, which are close to densely populated areas, have similar trends and values that are slightly higher than in FX-3 (Fig. 5). This may indicate that greater intensity in human activity played a role in promoting the burial of autochthonous OC. During the more natural evolutionary stage (1910–1950), sedimentation rates were low and relatively stable. OC burial in the lake sediments was largely dominated by autochthonous sources, with $OCAR_{auto}$ of 1.53 g C m^{-2} yr^{-1} pre-1950 (Fig. 5). However, during economic transformations (1950–2017) following the founding of the new China, average $OCAR_{auto}$ increased to 10.56 g C m^{-2} yr^{-1}. In particular, $OCAR_{auto}$ increased rapidly after 1980s (following introduction of the Reform and Opening Policies in 1978), to a mean $OCAR_{auto}$ of 13.11 g C m^{-2} yr^{-1}. Again after 2000, it increased to a mean $OCAR_{auto}$ of 16.76 g C m^{-2} yr^{-1} due to strong land-use/land-cover change in the lake watershed (e.g., about 30% increase in cultivated land, Li et al., 2017). The post-1950 $OCAR_{auto}$ was about 6.90 times that pre-1950. These observations indicate that human activities and/or climate changes during the past century have increased OC burial in lakes. Recent studies comparing post-1950 with 1850–1950, have found that OCAR increased 1.5 times in European lakes (Anderson et al., 2014), and by a factor of 1.6–4 in lakes of North America (Anderson et al., 2013; Dietz et al., 2015; Heathcote et al., 2015), all considered to be related to direct or indirect human impacts on lakes.

5.3. Impacts of climate and land-use changes on autochthonous OCAR

5.3.1. Response to climate change

The contemporary increase of $OCAR_{auto}$ in Fuxian Lake might be related to climatic factors such as temperature change (Brothers et al.,

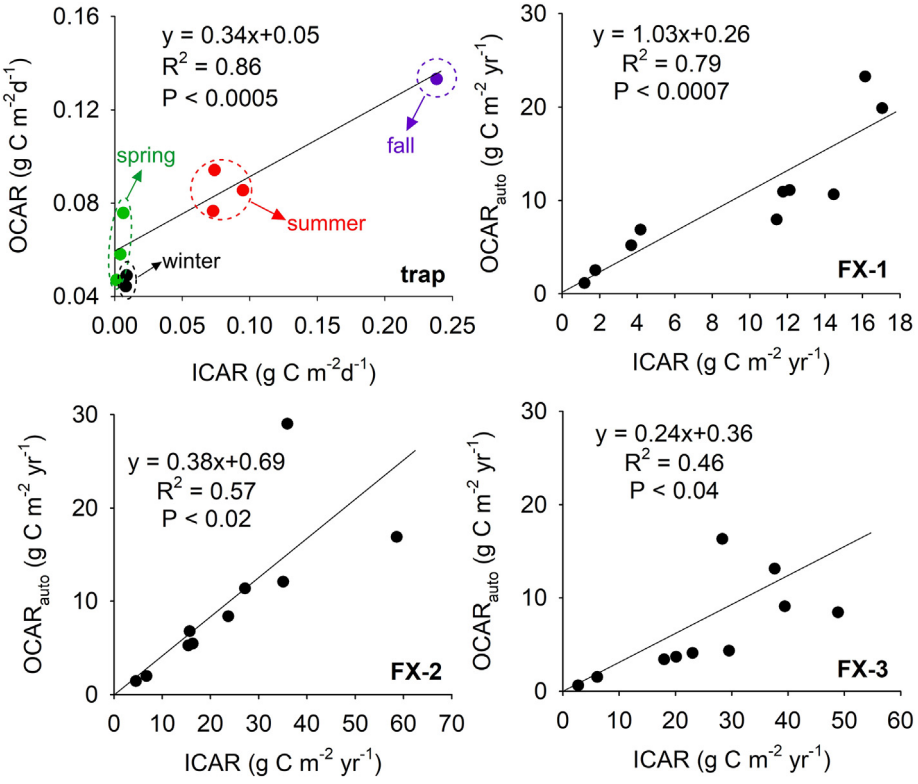

Fig. 7. The relationships between OCAR (or $OCAR_{auto}$) and ICAR (inorganic carbon accumulation rate) in the trap sediments during the monitoring year, 1/2017–1/2018, and OCAR and ICAR relationships in the individual cores FX-1, FX-2, FX-3, Fuxian Lake.

2008; Huang et al., 2017; Sobek et al., 2014), though the post-depositional mineralization rates were also temperature-dependent (Gudasz et al., 2010). In this study, OCAR ($OCAR_{auto}$-dominated) in the trap samples reached their maximum in summer and fall (Fig. 7), suggesting that enhancement of the BCP effect by temperature increase may be important. In the core sediments, there was no relationship between $OCAR_{auto}$ and rainfall amounts, but a statistically significant positive relationship between $OCAR_{auto}$ and temperature (Fig. 8). The mean annual air temperature at Fuxian Lake rose from 15.1 °C to 17.2 °C between 1961 and 2017. $OCAR_{auto}$ increased by 6.15 g C m^{-2} yr^{-1} per 1 °C increase in temperature. Therefore, a significant growth in $OCAR_{auto}$ is related to the global warming. In addition, the increasing alkalinity production and export may be related to the increase in surface air temperature (Drake et al., 2018). This process increases the concentration of DIC entering the lake, which may act as a nourishment to the aquatic plants and promote more OC burial. It is clear that lakes are acting as sentinels and integrators of regional processes.

5.3.2. Response to land-use change

Changes in land-use patterns have to be considered one of the most significant human activities affecting lake organic carbon (Anderson et al., 2013). Agriculture is clearly the dominant control of OCAR in many lakes (Anderson et al., 2013; Huang et al., 2017). The conversion of forested land to agriculture increases soil erosion, more nutrients are released by soil leaching, leading to the enrichment of nitrogen and phosphorus nutrients and increased production of organic matter (Schelske et al., 1988). In addition, a study in Mississippi River showed that the increase in bicarbonate and water fluxes was caused mainly by an increase in discharge from agricultural watersheds (Raymond et al., 2008), which may fertilize the aquatic photosynthesis and increase the burial efficiency of thus formed OC by the BCP effect (Chen et al., 2017; Liu et al., 2018; Yang et al., 2016).

In the Fuxian Lake basin, there has been continuous decrease in forest area, increase in population density and cultivated area, during the past 40 years (Li et al., 2017). Average $OCAR_{auto}$ in the lake showed continued increase (Fig. 5). There was a high correlation between $OCAR_{auto}$ and land-cover conversion (forest area, $R^2 = 0.43$, $P < 0.01$, $n = 15$; cultivated area, $R^2 = 0.34$, $P < 0.003$, $n = 15$) or total nitrogen ($R^2 = 0.52$, $P < 0.0001$, $n = 30$) (Fig. 9). Consequently, $OCAR_{auto}$ for the catchments with deforestation and developed agriculture was higher than it was during the period of little-disturbed natural evolution. Anderson et al. (2013) even concluded that land-use change, not climate, controls organic carbon burial in lakes. Unfortunately, this study did not distinguish between allochthonous and autochthonous organic carbon burial, which is needed to understand the carbon cycle and underlying mechanisms in detail, in order to help mitigate the impact of future climate change.

Tranvik et al. (2009) estimated that approximately 0.6 Pg C yr^{-1} is buried in lakes and reservoirs sediments. If the lowest value of proportion of autochthonous source of OC in the core sediments at Fuxian Lake, 47% (Table 3), was taken, then 0.28 Pg C yr^{-1} is obtained, which is close to the estimated value (0.27 Pg C yr^{-1}) that buried by BCP effect on the terrestrial surface water system (lakes, reservoirs, etc.) (Liu et al., 2018), showing that the carbon sink by the coupled carbonate weathering with aquatic photosynthesis mechanism (CCW) may be an important control against global warming.

6. Conclusions

To understand the sensitivity of the CCW carbon sink mechanism to climate and land-use changes, a systematic study of trap and lake bottom core sediments was conducted in Fuxian Lake (Yunnan, SW China), the second-deepest freshwater lake in China. The following conclusions are drawn:

(1) Autochthonous OC in the Fuxian Lake sediments was characterized by lower C/N ratio and higher $\delta^{13}C_{org}$. By determining the n-alkane distributions, the proportion of autochthonous OC was found to be in the range of 60–68%, indicating that BCP effect plays an important role in the stability of carbonate weathering carbon sink;
(2) The increase in the accumulation rate of autochthonous OC ($OCAR_{auto}$) was accompanied by an increase in the inorganic carbon accumulation rate (ICAR) in both the trap and core sediment samples. Particularly important was the determination that the post-1950 $OCAR_{auto}$ was about 6.9 times that for the previous period, 1910–1950, suggesting that the greater intensity in human activity may have a great impact on the burial of autochthonous OC;
(3) $OCAR_{auto}$ in the core sediments has increased significantly with global warming and land-use change, from 1.06 g C m^{-2} yr^{-1} in 1910 to 21.74 g C m^{-2} yr^{-1} in 2017. This increasing carbon sink may act as a negative feedback on global warming if the trend holds for all the lakes in the world.

This study is believed to be the first to quantify the flux of organic carbon buried by the BCP effect (i.e., the autochthonous organic carbon) in a lake. We need more comprehensive and in-depth works on a global scale to resolve the problem of the missing carbon sink in the global carbon cycle.

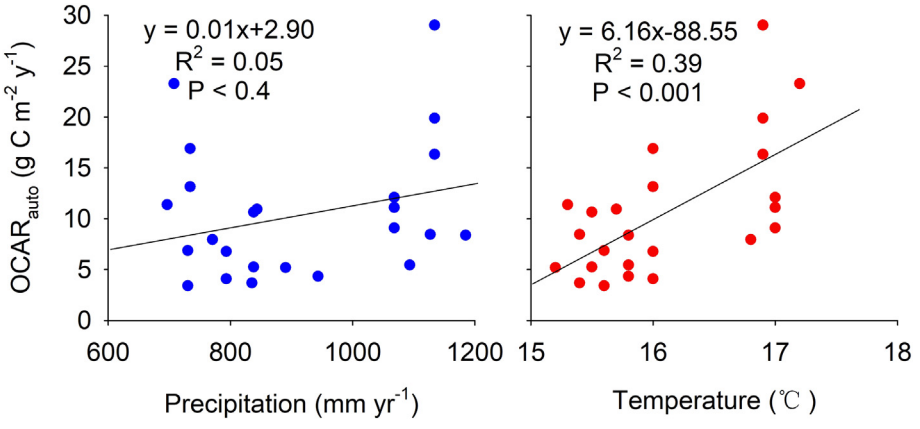

Fig. 8. Plots of $OCAR_{auto}$ and mean monthly precipitation and temperature, ($n = 24$) at Fuxian lake. Data from the China Meteorological Administration: http://www.cma.gov.cn/.

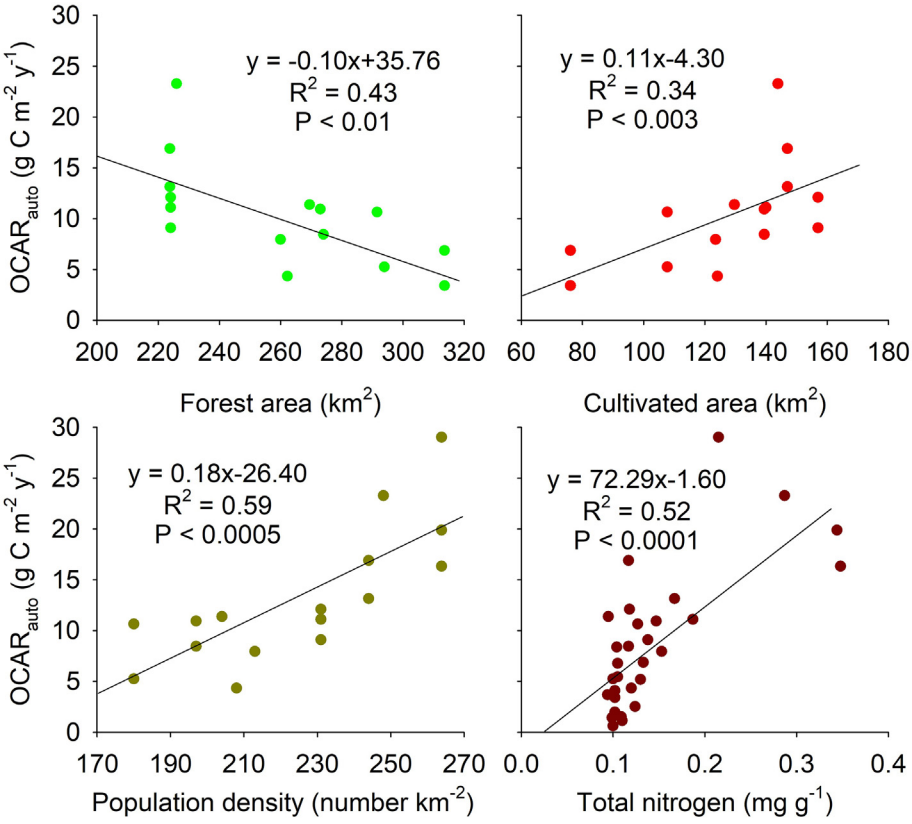

Fig. 9. The relationships between $OCAR_{auto}$ and selected limnological variables (total nitrogen, n = 30, this study; land-use of forest and cultivated area, n = 15; population density, n = 16, Li et al. (2017); Yunnan Provincial Bureau of Statistics: http://www.stats.yn.gov.cn/).

Declaration of competing interest

We declare that we have no financial and personal relationships with other people or organizations that can inappropriately influence our work.

Acknowledgements

This work was supported by the National Natural Science Foundation of China (U1612441 and 41921004) and the Strategic Priority Research Program of Chinese Academy of Sciences (Grant No. XDB 40020000). Special thanks are given to Prof. Dr. Derek Ford (McMaster University, Canada) for his thoughtful comments and corrections, which greatly improved the original draft.

References

Anderson, N.J., Dietz, R.D., Engstrom, D.R., 2013. Land-use change, not climate, controls organic carbon burial in lakes. Proc. Roy. Soc. London B: Biol. Sci. 280, 20131278.
Anderson, N.J., Bennion, H., Lotter, A.F., 2014. Lake eutrophication and its implications for organic carbon sequestration in Europe. Glob. Change Biol. 20, 2741–2751.
Appleby, P.G., 2002. Chronostratigraphic techniques in recent sediments. Tracking Environmental Change Using Lake Sediments. Springer, Dordrecht, pp. 171–203.
Appleby, P.G., 2008. Three decades of dating recent sediments by fallout radionuclides: a review. Holocene 18, 83–93.
Battin, T.J., Luyssaert, S., Kaplan, L.A., Aufdenkampe, A.K., Richter, A., Tranvik, L.J., 2009. The boundless carbon cycle. Nat. Geosci. 2, 598–600.
Beaulieu, E., Goddéris, Y., Donnadieu, Y., Labat, D., Roelandt, C., 2012. High sensitivity of the continental-weathering carbon dioxide sink to future climate change. Nat. Clim. Chang. 2, 346–349.
Berner, R.A., 2003. The long-term carbon cycle, fossil fuels and atmospheric composition. Nature 426, 323–326.
Bianchi, T.S., 2007. Biogeochemistry of Estuaries. Oxford University Press, London.
Blumer, M., Guillard, R.R.L., Chase, T., 1971. Hydrocarbons of marine phytoplankton. Mar. Biol. 8, 183–189.
Bourbonniere, R.A., Meyers, P.A., 1996. Sedimentary geolipid records of historical changes in the watersheds and productivities of Lakes Ontario and Erie. Limnol. Oceanogr. 41, 352–359.
Broecker, W.S., Takahashi, T., Simpson, H.J., Peng, T.H., 1979. Fate of fossil fuel carbon dioxide and the global carbon budget. Science 206, 409–418.
Brothers, S., Vermaire, J.C., Gregory-Eaves, I., 2008. Empirical models for describing recent sedimentation rates in lakes distributed across broad spatial scales. J. Paleolimnol. 40, 1003–1019.
Buffam, I., Turner, M.G., Desai, A.R., Hanson, P.C., Rusak, J.A., Lottig, N.R., Stanley, E.H., Carpenter, S.R., 2011. Integrating aquatic and terrestrial components to construct a complete carbon budget for a north temperate lake district. Glob. Change Biol. 17, 1193–1211.
Canuel, E.A., Freeman, K.H., Wakeham, S.G., 1997. Isotopic compositions of lipid biomarker compounds in estuarine plants and surface sediments. Limnol. Oceanogr. 42, 1570–1583.
Chen, J., Wan, G., Wang, F., Zhang, D., Huang, R., Zhang, F., Schmidt, R., 2002. Environmental records of carbon in recent lake sediments. Sci. China Ser. D Earth Sci. 45, 875–884.
Chen, X., Chen, G., Lu, H., Liu, X., Zhang, H., 2015. Long-term diatom biodiversity responses to productivity in lakes of Fuxian and Dianchi. Biodivers. Sci. 23, 89–100 (in Chinese).
Chen, B., Yang, R., Liu, Z., Sun, H., Yan, H., Zeng, Q., Zeng, S., Zeng, C., Zhao, M., 2017. Coupled control of land uses and aquatic biological processes on the diurnal hydrochemical variations in the five ponds at the Shawan Karst Test Site, China: implications for the carbonate weathering-related carbon sink. Chem. Geol. 456, 58–71.
Chen, J., Yang, H., Zeng, Y., Guo, J., Song, Y., Ding, W., 2018. Combined use of radiocarbon and stable carbon isotope to constrain the sources and cycling of particulate organic carbon in a large freshwater lake, China. Sci. Tot. Environ. 625, 27–38.
Ciais, P., et al., 2013. Carbon and other biogeochemical cycles. In: Stocker, T.F. (Ed.), Climate Change 2013: The Physical Science Basis. Contribution of Working Group I to the Fifth Assessment Report of the Intergovernmental Panel on Climate Change. Cambridge University Press, Cambridge, United Kingdom and New York, NY, USA, pp. 465–570.
Clow, D.W., Stackpoole, S.M., Verdin, K.L., Butman, D.E., Zhu, Z., Krabbenhoft, D.P., Striegl, R.G., 2015. Organic carbon burial in lakes and reservoirs of the conterminous United States. Environ. Sci. Technol. 49, 7614–7622.
Cole, J.J., Prairie, Y.T., Caraco, N.F., McDowell, W.H., Tranvik, L.J., Striegl, R.G., Duarte, C.M., Kortelainen, P., Downing, J.A., Middelburg, J.J., Melack, J., 2007. Plumbing the global carbon cycle: integrating inland waters into the terrestrial carbon budget. Ecosystems 10, 172–185.
Cui, Y.D., Liu, X.Q., Wang, H.Z., 2008. Macrozoobenthic community of Fuxian Lake, the deepest lake of Southwest China. Limnol.-Ecol. Man. Inland Water. 38, 116–125.
Dean, W.E., 1999. The carbon cycle and biogeochemical dynamics in lake sediments. J. Paleolimnol. 21, 375–393.
Dean, W.E., Gorham, E., 1998. Magnitude and significance of carbon burial in lakes, reservoirs, and peatlands. Geology 26, 535–538.

Dietz, R.D., Engstrom, D.R., Anderson, N.J., 2015. Patterns and drivers of change in organic carbon burial across a diverse landscape: insights from 116 Minnesota lakes. Glob. Biogeochem. Cy. 29, 708–727.

Dittrich, M., Obst, M., 2004. Are picoplankton responsible for calcite precipitation in lakes? AMBIO 33, 559–564.

Dong, X.H., Anderson, N.J., Yang, X.D., Chen, X., Shen, J., 2012. Carbon burial by shallow lakes on the Yangtze floodplain and its relevance to regional carbon sequestration. Glob. Change Biol. 18, 2205–2217.

Downing, J.A., Cole, J.J., Middelburg, J.J., Striegl, R.G., Duarte, C.M., Kortelainen, P., Prairie, Y.T., Laube, K.A., 2008. Sediment organic carbon burial in agriculturally eutrophic impoundments over the last century. Glob. Biogeochem. Cy. 22, GB1018.

Drake, T.W., Tank, S.E., Zhulidov, A.V., Holmes, R.M., Gurtovaya, T., Spencer, R.G., 2018. Increasing alkalinity export from large Russian arctic rivers. Environ. Sci. Technol. 52, 8302–8308.

Dreybrodt, W., 1988. Processes in Karst Systems. Springer, Berlin.

Eglinton, G., Hamilton, R.J., 1967. Leaf epicuticular waxes. Science 156, 1322–1335.

Einsele, G., Yan, J., Hinderer, M., 2001. Atmospheric carbon burial in modern lake basins and its significance for the global carbon budget. Glob. Planet. Change 30, 167–195.

Falkowski, P.G., Raven, J.A., 1997. Aquatic Photosynthesis. Blackwell Science, Oxford.

Ficken, K.J., Li, B., Swain, D.L., Eglinton, G., 2000. An n-alkane proxy for the sedimentary input of submerged/floating freshwater aquatic macrophytes. Org. Geochem. 31, 745–749.

Fokin, A.A., Chernish, L.V., Gunchenko, P.A., Tikhonchuk, E.Y., Hausmann, H., Serafin, M., Dahl, J.E.P., Carlson, R.M.K., Schreiner, P.R., 2012. Stable alkanes containing very long carbon–carbon bonds. J. Am. Chem. Soc. 134, 13641–13650.

Giger, W., Schaffner, C., Wakeham, S.G., 1980. Aliphatic and olefinic hydrocarbons in recent sediments of Greifensee, Switzerland. Geochim. Cosmochim. Acta 44, 119–129.

Gudasz, C., Bastviken, D., Steger, K., Premke, K., Sobek, S., Tranvik, L.J., 2010. Temperature-controlled organic carbon mineralization in lake sediments. Nature 466, 478–U3.

Gui, Z.F., Xue, B., Yao, S.C., Wei, W.J., Yi, S., 2013. Organic carbon burial in lake sediments in the middle and lower reaches of the Yangtze River Basin, China. Hydrobiologia 710, 143–156.

Guo, W., 2016. Source and Biogeochemical Properties of Organic Carbon in Water Column and Sediments of Pearl River Estuary. Ph D dissertation. University of Chinese Academy of Sciences (in Chinese).

Heathcote, A.J., Downing, J.A., 2012. Impacts of eutrophication on carbon burial in freshwater lakes in an intensively agricultural landscape. Ecosystems 15, 60–70.

Heathcote, A.J., Anderson, N.J., Prairie, Y.T., Engstrom, D.R., Del Giorgio, P.A., 2015. Large increases in carbon burial in northern lakes during the Anthropocene. Nature Comm. 6, 10016.

Huang, C., Yao, L., Zhang, Y., Huang, T., Zhang, M., Zhu, A.X., Yang, H., 2017. Spatial and temporal variation in autochthonous and allochthonous contributors to increased organic carbon and nitrogen burial in a plateau lake. Sci. Total Environ. 603, 390–400.

Huang, C., Zhang, L., Li, Y., Lin, C., Huang, T., Zhang, M., Zhu, A.X., Yang, H., Wang, X., 2018. Carbon and nitrogen burial in a plateau lake during eutrophication and phytoplankton blooms. Sci. Total Environ. 616, 296–304.

Jeng, W.L., 2006. Higher plant n-alkane average chain length as an indicator of petrogenic hydrocarbon contamination in marine sediments. Mar. Chem. 102, 242–251.

Kastowski, M., Hinderer, M., Vecsei, A., 2011. Long-term carbon burial in European lakes: analysis and estimate. Glob. Biogeochem. Cy. 25, GB3019.

Kelley, C.A., Coffin, R.B., Cifuentes, L.A., 1998. Stable isotope evidence for alternative bacterial carbon sources in the Gulf of Mexico. Limnol. Oceanogr. 43, 1962–1969.

Kelts, K., Hsü, K.J., 1978. Freshwater carbonate sedimentation. Lakes. Springer, New York, NY, pp. 295–323.

Kirchner, G., Ehlers, H., 1998. Sediment geochronology in changing coastal environments: potentials and limitations of the ^{137}Cs and ^{210}Pb methods. J. Coast. Res. 14, 483–492.

Lerman, A., Mackenzie, F.T., 2005. CO_2 air–sea exchange due to calcium carbonate and organic matter storage, and its implications for the global carbon cycle. Aquat. Geochem. 11, 345–390.

Li, G., Elderfield, H., 2013. Evolution of carbon cycle over the past 100 million years. Geochim. Cosmochim. Acta 103, 11–25.

Li, Y., Gong, Z., Xia, W., Shen, J., 2011. Effects of eutrophication and fish yield on the diatom community in Lake Fuxian, a deep oligotrophic lake in Southwest China. Diat. Res. 26, 51–56.

Li, S.H., Jin, B.X., Zhou, J.S., Wang, J.L., Peng, S.Y., 2017. Analysis of the spatiotemporal land-use/land-cover change and its driving forces in Fuxian Lake Watershed, 1974 to 2014. Polish J. Environ. Studies 26, 671–681.

Liu, Y., Wu, G., Gao, Z., 2008. Impacts of land-use change in Fuxian and Qilu basins of Yunnan Province on lake water quality. Chin. J. Ecol. 27, 447–453.

Liu, G., Liu, Z., Li, Y., Chen, F., Gu, B., Smoak, J.M., 2009. Effects of fish introduction and eutrophication on the cladoceran community in Lake Fuxian, a deep oligotrophic lake in Southwest China. J. Paleolimnol. 42, 427–435.

Liu, Z., Dreybrodt, W., Wang, H., 2010. A new direction in effective accounting for the atmospheric CO_2 budget: considering the combined action of carbonate dissolution, the global water cycle and photosynthetic uptake of DIC by aquatic organisms. Earth-Sci. Rev. 99, 162–172.

Liu, Z., Dreybrodt, W., Liu, H., 2011. Atmospheric CO_2 sink: silicate weathering or carbonate weathering? Appl. Geochem. 26, 292–294.

Liu, W., Li, X., An, Z., Xu, L., Zhang, Q., 2013. Total organic carbon isotopes: a novel proxy of lake level from Lake Qinghai in the Qinghai–Tibet Plateau, China. Chem. Geol. 347, 153–160.

Liu, H., Liu, Z., Macpherson, G.L., Yang, R., Chen, B., Sun, H., 2015. Diurnal hydrochemical variations in a karst spring and two ponds, Maolan Karst Experimental Site, China: biological pump effects. J. Hydrol. 522, 407–417.

Liu, Z., Macpherson, G.L., Groves, C., Martin, J.B., Yuan, D., Zeng, S., 2018. Large and active CO_2 uptake by coupled carbonate weathering. Earth-Sci. Rev. 182, 42–49.

Maavara, T., Lauerwald, R., Regnier, P., Van Cappellen, P., 2017. Global perturbation of organic carbon cycling by river damming. Nature Comm. 8, 15347.

Melnikov, N.B., O'Neill, B.C., 2006. Learning about the carbon cycle from global budget data. Geophys. Res. Lett. 33, L02705.

Mendonça, R., Kosten, S., Sobek, S., Cardoso, S.J., Figueiredo-Barros, M.P., Estrada, C.H.D., Roland, F., 2016. Organic carbon burial efficiency in a subtropical hydroelectric reservoir. Biogeosciences 13, 3331–3342.

Mendonça, R., Müller, R.A., Clow, D., Verpoorter, C., Raymond, P., Tranvik, L.J., Sobek, S., 2017. Organic carbon burial in global lakes and reservoirs. Nature Comm. 8, 1694.

Meyer, K.M., Yu, M., Lehrmann, D., Van de Schootbrugge, B., Payne, J.L., 2013. Constraints on Early Triassic carbon cycle dynamics from paired organic and inorganic carbon isotope records. Earth Planet. Sci. Lett. 361, 429–435.

Meyers, P.A., 1994. Preservation of elemental and isotopic source identification of sedimentary organic matter. Chem. Geol. 114, 289–302.

Meyers, P.A., 1997. Organic geochemical proxies of paleoceanographic, paleolimnologic, and paleoclimatic processes. Org. Geochem. 27, 213–250.

Meyers, P.A., 2003. Applications of organic geochemistry to paleolimnological reconstructions: a summary of examples from the Laurentian Great Lakes. Org. Geochem. 34, 261–289.

Meyers, P.A., Ishiwatari, R., 1993. Lacustrine organic geochemistry—an overview of indicators of organic matter sources and diagenesis in lake sediments. Org. Geochem. 20, 867–900.

Mortillaro, J.M., Abril, G., Moreira-Turcq, P., Sobrinho, R.L., Perez, M., Meziane, T., 2011. Fatty acid and stable isotope (δ^{13}C, δ^{15}N) signatures of particulate organic matter in the lower Amazon River: seasonal contrasts and connectivity between floodplain lakes and the mainstem. Org. Geochem. 42, 1159–1168.

Nõges, P., Cremona, F., Laas, A., Martma, T., Rõõm, E.I., Toming, K., Viik, M., Vilbaste, S., Nõges, T., 2016. Role of a productive lake in carbon sequestration within a calcareous catchment. Sci. Total Environ. 550, 225–230.

Ogura, K., Machihara, T., Takada, H., 1990. Diagenesis of biomarkers in Biwa lake sediments over 1 million years. Org. Geochem. 16, 805–813.

O'Reilly, S.S., Szpak, M.T., Flanagan, P.V., Monteys, X., Murphy, B.T., Jordan, S.F., Allen, C.C.R., Simpson, A.J., Mulligan, S.M., Sandron, S., Kelleher, B.P., 2014. Biomarkers reveal the effects of hydrography on the sources and fate of marine and terrestrial organic matter in the western Irish Sea. Estuar. Coast. Shelf Sci. 136, 157–171.

Ortiz, J.E., Díaz-Bautista, A., Aldasoro, J.J., Torres, T., Gallego, J.L.R., Moreno, L., Estébanez, B., 2011. n-Alkan-2-ones in peat-forming plants from the Roñanzas ombrotrophic bog (Asturias, northern Spain). Org. Geochem. 42, 586–592.

Poynter, J., Eglinton, G., 1990. Molecular composition of three sediments from hole 717c: the Bengal fan. Proceedings of the Ocean Drilling Program: Scientific Results. 116, pp. 155–161.

Ramaswamy, V., Gaye, B., Shirodkar, P.V., Rao, P.S., Chivas, A.R., Wheeler, D., Thwin, S., 2008. Distribution and sources of organic carbon, nitrogen and their isotopic signatures in sediments from the Ayeyarwady (Irrawaddy) continental shelf, northern Andaman Sea. Mar. Chem. 111, 137–150.

Rao, Z., Jia, G., Qiang, M., Zhao, Y., 2014. Assessment of the difference between mid-and long chain compound specific delta Dn-alkanes values in lacustrine sediments as a paleoclimatic indicator. Org. Geochem. 76, 104–117.

Raymond, P.A., Oh, N.H., Turner, R.E., Broussard, W., 2008. Anthropogenically enhanced fluxes of water and carbon from the Mississippi River. Nature 451, 449–452.

Regnier, P., et al., 2013. Anthropogenic perturbation of the carbon fluxes from land to ocean. Nat. Geosci. 6, 597–607.

Riebesell, U., Schulz, K.G., Bellerby, R.G.J., Botros, M., Fritsche, P., Meyerhöfer, M., Neill, C., Nondal, G., Oschlies, A., Wohlers, J., Zöllner, E., 2007. Enhanced biological carbon consumption in a high CO_2 ocean. Nature 450, 545–U10.

Sanchez-Cabeza, J.A., Ruiz-Fernández, A.C., 2012. ^{210}Pb sediment radiochronology: an integrated formulation and classification of dating models. Geochim. Cosmochim. Acta 82, 183–200.

Schefuß, E., Ratmeyer, V., Stuut, J.B.W., Jansen, J.F., Damsté, J.S.S., 2003. Carbon isotope analyses of n-alkanes in dust from the lower atmosphere over the central eastern Atlantic. Geochim. Cosmochim. Acta 67, 1757–1767.

Schelske, C.L., Robbins, J.A., Gardner, W.S., Conley, D.J., Bourbonniere, R.A., 1988. Sediment record of biogeochemical responses to anthropogenic perturbations of nutrient cycles in Lake Ontario. Can. J. Fish. Aquat. Sci. 45, 1291–1303.

Schindler, D.W., 1999. Carbon cycling: the mysterious missing sink. Nature 398, 105.

Seki, O., Yoshikawa, C., Nakatsuka, T., Kawamura, K., Wakatsuchi, M., 2006. Fluxes, source and transport of organic matter in the western Sea of Okhotsk: stable carbon isotopic ratios of n-alkanes and total organic carbon. Deep Sea Res. 53, 253–270.

Sikes, E.L., Uhle, M.E., Nodder, S.D., Howard, M.E., 2009. Sources of organic matter in a coastal marine environment: evidence from n-alkanes and their δ^{13}C distributions in the Hauraki Gulf, New Zealand. Mar. Chem. 113, 149–163.

Silva, T.R., Lopes, S.R., Spörl, G., Knoppers, B.A., Azevedo, D.A., 2012. Source characterization using molecular distribution and stable carbon isotopic composition of n-alkanes in sediment cores from the tropical Mundaú–Manguaba estuarine–lagoon system. Brazil. Org. Geochem. 53, 25–33.

Snedaker, S.C., Glynn, P.W., Rumbold, D.G., Corcoran, E.F., 1995. Distribution of n-alkanes in marine samples from Southeast Florida. Mar. Poll. Bull. 30, 83–89.

Sobek, S., Anderson, N.J., Bernasconi, S.M., Del Sontro, T., 2014. Low organic carbon burial efficiency in arctic lake sediments. J. Geophys. Res. Biogeosci. 119, 1231–1243.

Sojinu, O.S., Wang, J.Z., Sonibare, O.O., Zeng, E.Y., 2010. Polycyclic aromatic hydrocarbons in sediments and soils from oil exploration areas of the Niger Delta, Nigeria. J. Hazard. Mat. 174, 641–647.

Sun, H.G., Han, J.T., Zhang, S.R., Lu, X.X., 2011. Transformation of dissolved inorganic carbon (DIC) into particulate organic carbon (POC) in the lower Xijiang River, SE China: an isotopic approach. Biogeosci. Discuss. 8, 9471–9501.

Sundquist, E.T., 1993. The global carbon dioxide budget. Science 259, 934–941.

Tans, P.P., Fung, I.Y., Takahashi, T., 1990. Observational constraints on the global atmospheric CO_2 budget. Science 247, 1431–1438.
Tareq, S.M., Tanoue, E., Tsuji, H., Tanaka, N., Ohta, K., 2005. Hydrocarbon and elemental carbon signatures in a tropical wetland: biogeochemical evidence of forest fire and vegetation changes. Chemosphere 59, 1655–1665.
Ternon, J.F., Oudot, C., Dessier, A., Diverres, D., 2000. A seasonal tropical sink for atmospheric CO_2 in the Atlantic Ocean: the role of the Amazon River discharge. Mar. Chem. 68, 183–201.
Tolosa, I., de Mora, S., Sheikholeslami, M.R., Villeneuve, J.P., Bartocci, J., Cattini, C., 2004. Aliphatic and aromatic hydrocarbons in coastal Caspian Sea sediments. Mar. Poll. Bull. 48, 44–60.
Tranvik, L.J., Downing, J.A., Cotner, J.B., et al., 2009. Lakes and reservoirs as regulators of carbon cycling and climate. Limnol. Oceanogr. 54, 2298–2314.
Tue, N.T., Hamaoka, H., Sogabe, A., Quy, T.D., Nhuan, M.T., Omori, K., 2011. The application of $\delta^{13}C$ and C/N ratios as indicators of organic carbon sources and paleoenvironmental change of the mangrove ecosystem from Ba Lat Estuary, Red River, Vietnam. Environ. Earth Sci. 64, 1475–1486.
Tyson, R.V., 2012. Sedimentary Organic Matter: Organic Facies and Palynofacies (Springer Science & Business Media).
Verburg, P., 2007. The need to correct for the Sueiss effect in the application of $\delta^{13}C$ in sediment of autotrophic Lake Tanganyika, as a productivity proxy in the Anthropocene. J. Paleolimnol. 37, 591–602.
Viso, A.C., Pesando, D., Bernard, P., Marty, J.C., 1993. Lipid components of the Mediterranean seagrass Posidonia oceanica. Phytochemistry 34, 381–387.
Volkman, J.K., Johns, R.B., Gillan, F.T., Perry, G.J., Bavor Jr., H.J., 1980. Microbial lipids of an intertidal sediment—I. Fatty acids and hydrocarbons. Geochim. Cosmochim. Acta 44, 1133–1143.
Walker, J.C., Hays, P.B., Kasting, J.F., 1981. A negative feedback mechanism for the long term stabilization of Earth's surface temperature. J. Geophys. Res. 86, 9776–9782.
Wang, S., Dou, H., 1998. China Lakes Chorography. Science press, Beijing (in Chinese).
Wang, Z., Liu, W., 2012. Carbon chain length distribution in n-alkyl lipids: a process for evaluating source inputs to Lake Qinghai. Org. Geochem. 50, 36–43.
Wang, X., Yang, H., Gu, Z., Zhang, M., Yang, B., 2018. A century of change in sediment accumulation and trophic status in Lake Fuxian, a deep plateau lake of Southwestern China. J. Soil. Sed. 18, 1133–1146.
Waterson, E.J., Canuel, E.A., 2008. Sources of sedimentary organic matter in the Mississippi River and adjacent Gulf of Mexico as revealed by lipid biomarker and $\delta^{13}C_{TOC}$ analyses. Org. Geochem. 39, 422–439.
White, A.F., Brantley, S.L., 2003. The effect of time on the weathering of silicate minerals: why do weathering rates differ in the laboratory and field? Chem. Geol. 202, 479–506.
Yang, M., Liu, Z., Sun, H., Yang, R., Chen, B., 2016. Organic carbon source tracing and DIC fertilization effect in the Pearl River: insights from lipid biomarker and geochemical analysis. Appl. Geochem. 73, 132–141.
Yu, Z.T., Wang, X.J., Zhao, C.Y., Lan, H.Y., 2015. Carbon burial in Bosten Lake over the past century: impacts of climate change and human activity. Chem. Geol. 419, 132–141.
Zeng, S., Liu, H., Chen, B., Liu, Z., Zeng, C., Min, Z., Sun, H., Zeng, Q., Yang, R., Yang, M., Hu, Y., 2019a. Seasonal and diurnal variations in DIC, NO_3^- and TOC concentrations of spring-pond ecosystems under different land-uses at Shawan Karst Test Site, SW China: carbon limitation of aquatic photosynthesis. J. Hydrol. 574, 811–821.
Zeng, S., Liu, Z., Kaufmann, G., 2019b. Sensitivity of the global carbonate weathering carbon-sink flux to climate and land-use changes. Nature Comm. 10, 1–10.
Zhang, Z., Zhao, M., Yang, X., Wang, S., Jiang, X., Oldfield, F., Eglinton, G., 2004. A hydrocarbon biomarker record for the last 40 kyr of plant input to Lake Heqing, southwestern China. Org. Geochem. 35, 595–613.
Zhang, Y., Su, Y., Liu, Z., Chen, X., Yu, J., Di, X., Miao, J., 2015. Sediment lipid biomarkers record increased eutrophication in Lake Fuxian (China) during the past 150 years. J. Great Lakes Res. 41, 30–40.
Zhang, F., Yao, S., Xue, B., Lu, X., Gui, Z., 2017. Organic carbon burial in Chinese lakes over the past 150 years. Quat. Int. 438, 94–103.
Zhang, F., Xue, B., Yao, S., Gui, Z., 2018. Organic carbon burial from multi-core records in Hulun Lake, the largest lake in northern China. Quat. Int. 475, 80–90.
Zheng, Y., Zhou, W., Meyers, P.A., Xie, S., 2007. Lipid biomarkers in the Zoigê-Hongyuan peat deposit: indicators of Holocene climate changes in West China. Org. Geochem. 38, 1927–1940.